Atmos. Meas. Tech. Discuss., 7, 1535–1572, 2014
www.atmos-meas-tech-discuss.net/7/1535/2014/
doi:10.5194/amtd-7-1535-2014

Atmospheric Measurement Techniques
Discussions
Open Access

Gimballed Limb Observer for Radiance Imaging of the Atmosphere (GLORIA) scientific objectives

M. Riese[1], H. Oelhaf[2], P. Preusse[1], J. Blank[1], M. Ern[1], F. Friedl-Vallon[2], H. Fischer[2], T. Guggenmoser[1], M. Höpfner[2], P. Hoor[3], M. Kaufmann[1], J. Orphal[2], F. Plöger[1], R. Spang[1], O. Suminska-Ebersoldt[2], J. Ungermann[1], B. Vogel[1], and W. Woiwode[2]

[1]Institute of Energy and Climate Research, Stratosphere (IEK-7), Forschungzentrum Jülich, 52425 Jülich, Germany
[2]Institute for Meteorology and Climate Research, Karlsruhe Institute of Technology, Karlsruhe, Germany
[3]Institute for Atmospheric Physics, University Mainz, Mainz, Germany

Received: 23 December 2013 – Accepted: 2 February 2014 – Published: 14 February 2014

Correspondence to: M. Riese (m.riese@fz-juelich.de)

Published by Copernicus Publications on behalf of the European Geosciences Union.

Abstract

The upper troposphere/lower stratosphere (UTLS) plays a crucial role in the climate system. Changes in the composition and dynamic structure of this atmospheric region result in particularly large changes in the atmospheric radiation balance. Quantifying the physical and chemical processes that control UTLS composition therefore represents an important task. Currently, there is a lack of UTLS observations with sufficient three-dimensional resolution. The Gimballed Limb Observer for Radiance Imaging of the Atmosphere (GLORIA) aircraft instrument addresses this observational lack by providing observations of numerous trace constituents as well as temperature and cloud structures with an unprecedented combination of vertical resolution (up to 300 m) and horizontal resolution (up to 20 km × 20 km). As a result, important scientific questions concerning stratosphere–troposphere-exchange, the occurrence of subvisible cirrus clouds in the lowermost stratosphere (LMS), polar chemistry and gravity wave processes can be addressed, as reviewed in this paper.

1 Introduction

Changes and variability of UTLS composition are major drivers of surface climate change (e.g., Solomon et al., 2007, 2010). Even small changes of spatially highly variable concentrations of greenhouse gases such as water vapour (H_2O) and ozone (O_3), aerosols and cirrus clouds have significant effects on the atmospheric radiation balance. Improved prediction capabilities of chemistry-climate models (CCM) therefore rely on a realistic representation of UTLS processes affecting UTLS composition.

UTLS composition is governed by the complex interactions of various physical and chemical processes that operate at a wide range of temporal and spatial scales (local to global) as illustrated in Fig. 1. Water vapour and ozone are particularly sensitive to atmospheric transport due to their steep spatial mixing ratio gradients in this region. Small-scale trace gas filaments in the UTLS represent an important example of

AMTD
7, 1535–1572, 2014

structures that are not yet adequately characterised. They arise from chaotic advection of tracers, driven by the large scale flow (Lorenz, 1963). Dissipation of these structures is associated with a scale collapse, which occurs in regions of strong wind shear rates. Riese et al. (2012) showed that even small uncertainties in this dissipation process (mixing strength) have a significant impact on simulated UTLS composition, for example on water vapour and ozone concentrations, and associated radiative effects (see Fig. 2).

In the past, most progress in our understanding of the UTLS and small-scale processes in this region has been made on the basis of detailed airborne in-situ observations. Satellite limb-observations, e.g. by the Michelson Interferometer for Passive Atmospheric Sounding (MIPAS) onboard Envisat (Fischer et al., 2008), provided the global view, however, at limited spatial resolution. Currently, there is a gap of observations concerning small-scale trace gas structures and temperature fluctuations, with a vertical extent of less than 500 m and a horizontal extent of less than 100 km. The Gimballed Limb Observer for Radiance Imaging of the Atmosphere (GLORIA) is designed to fill this gap by two- and three-dimensional observations with unprecedented spatial resolution.

This paper describes the scientific objectives of GLORIA. Section 2 gives a brief review of the history of infrared-limb sounding in terms of spatial and spectral resolution. A brief description of the advanced limb-imaging and tomographic capabilities of GLORIA is given in Sect. 3. In Sect. 4, we discuss important scientific questions in the area of UTLS composition and dynamics that will be addressed by GLORIA observations in the coming years. A short summary and conclusion is given in Sect. 5.

2 Infrared limb-sounding

Infrared limb-emission sounders measure the radiance emitted by the atmosphere along the line of sight (LOS) as illustrated in Fig. 3. The method provides high vertical resolution since the LOS segment for the layer above the tangent point (closest point to the Earth surface) is relatively large compared to other segments and the total density of the atmosphere exponentially decreases with altitude. Global observations of atmospheric infrared limb-emissions were therefore made by a number of low Earth-orbit satellite instruments in order to obtain vertically resolved profile data of temperature, a variety of trace gases, aerosols, and clouds simultaneously, at daytime and night-time (e.g., Drummond et al., 1980; Gille and Russel III, 1984; Roche et al., 1993; Taylor et al., 1993; Bingham et al., 1997; Offermann et al., 1999; Russell, 1999; Fischer et al., 2008; Gille et al., 2008). These satellite observations greatly contributed to our understanding of the 3-D chemical structure and large-scale dynamics of the middle atmosphere.

For improved horizontal resolution, the Cryogenic Infrared Spectrometers and Telescopes for the Atmosphere (CRISTA) instrument onboard the Shuttle Palette Satellite (SPAS) employed three telescopes that scanned the Earth horizon in the altitude range from 10 to 100 km at horizontal angles of 18° apart. By this approach, the large horizontal measurement gap between subsequent orbits, about 2000 km at the equator, could be filled and a horizontal across-track sampling of about 600 km was achieved. The along-track sampling was 200 to 400 km, depending on the measurement mode. CRISTA was successfully operated during two missions of NASA's Space Shuttle, STS66 in November 1994 (Offermann et al., 1999) and STS85 in August 1997 (Grossmann et al., 2002). During its one week missions, the instrument provided global snap shots of stratospheric and mesospheric temperature and about 10 trace gases (Riese et al., 1997, 1999a) with the best three-dimensional spatial resolution of global trace gas observations achieved up to date. Parts of the CRISTA optical system were later re-used on the high-flying Russian research aircraft M55-Geophysica by the CRISTA – New Frontiers (NF) instrument for limb-observations in the UTLS with unprecedented vertical resolution and along flight-track sampling (e.g., Kullmann et al., 2004; Ungermann et al., 2012).

To acquire the most complete set of composition data of the stratosphere, pole-to-pole over almost a full solar cycle, MIPAS on ESA's Envisat was focusing on high spectral rather than high spatial resolution. It was operating from 2002 until 2012. By observing the 4 to 15 µm range at very high spectral sampling, up to 40 atmospheric trace gases could be measured in the nominal altitude range from 6 to 68 km (in some modes extended up to 150 km) at 2 to 4 km vertical spacing and 300 to 500 km along-track sampling (Fischer et al., 2008). The development of MIPAS onboard Envisat was based on experience with the balloon-borne precursor MIPAS-B (Fischer and Oelhaf, 1996; Friedl-Vallon et al., 2004) and was later on complemented by the MIPAS-STR instrument onboard M55-Geophysica (e.g., Piesch et al., 1996; Woiwode et al., 2012).

A new scientific focus of infrared limb sounding is the region of the UTLS owing to its immense importance for the climate system. Airborne limb-emission sensors such as MIPAS-STR and CRISTA-NF provide adequate spatial sampling in the UTLS in two dimensions (vertical and along the flight track) but no spatial sampling in the viewing direction. Lidar observations typically measure two-dimensional curtains (vertical × flight direction) of a few atmospheric species such as H_2O or O_3. Many UTLS objectives require, however, precise three-dimensional observations of temperature and multiple trace gases with a vertical resolution better than 1 km and a horizontal resolution of a few 10s of km (e.g., ESA, 2012). To fulfill this requirement, the limb-imaging technique was proposed (Riese et al., 2005; Friedl-Vallon et al., 2006), which combines high spatial resolution in three-dimensions with high spectral resolution, i.e. a high number of detectable species.

The infrared limb-imaging technique basically combines two-dimensional detector arrays with Fourier Transform Spectroscopy (FTS) for about 10^3 to 10^4 simultaneous limb-views in the mid-infrared spectral region. The capabilities of this technique were studied for application on a satellite in the framework of the Earth Explorer (EE-7) program by the European Space Agency (ESA, 2012). It could be shown that global limb-imaging would result in a significant reduction of uncertainties in key physical and chemical processes in the atmosphere that are currently limiting the predictive capabilities of Earth system and climate models. The concept will therefore be further studied

AMTD
7, 1535–1572, 2014

in the framework of the ESA Earth Explorer programme and for a proposed German limb-imaging mission (ATMO-SAT).

3 Airborne infrared limb-imaging with GLORIA

Previous airborne limb-emission sounders such as MIPAS-STR and CRISTA-NF onboard the high-flying Russian aircraft M55-Geophysica measure multiple trace gases in the UTLS with high spatial sampling in two dimensions, vertically up to 200 m and up to 20 km along the flight track. These instruments were successfully employed during the tropical SCOUT-O3 aircraft campaign in 2005 (e.g., Spang et al., 2008; Hoffmann et al., 2009), in the framework of the tropical TROCCINOX and the ENVISAT validation campaigns (Keim et al., 2008), during AMMA-SCOUT in 2006 (e.g., Weigel et al., 2010, 2012; Ungermann et al., 2013), and during the Arctic RECONCILE aircraft campaign in 2010 (e.g., Woiwode et al., 2012; Kalicinsky et al., 2013; von Hobe et al., 2013).

While CRISTA-NF and MIPAS-STR provide excellent sampling and resolution along the flight track, the resolution perpendicular to the flight track is limited by the relative broad weighting functions (about 200 km) of the atmospheric radiative transfer. Also due to the single detector approach some measurement time is used up for scanning over the limb, resulting in an irregular sampling of the atmosphere. These limitations can be overcome by using a 2-D detector instead of single detectors, enabling limb-imaging instead of limb-scanning (Friedl-Vallon et al., 2014). In addition, this technique offers a way to get better information on the 3rd horizontal dimension (i.e. along the line-of-sight) by applying tomographic techniques. GLORIA represents the first realization of the infrared limb-imaging technique. Its first deployments took place onboard M55-Geophysica during the ESA Sounder Campaign 2011 (Essence-11) in December 2011 from Kiruna (Sweden). In summer/autumn 2012, GLORIA was deployed on HALO during the Transport and Composition in the UT/LMS (TACTS) and Earth System Model Validation (ESMVal) campaigns. Future aircraft campaigns are discussed in Sect. 4.

3.1 GLORIA instrument concept and measurement modes

GLORIA combines a classical Fourier transform spectrometer (FTS) with a 2-D detector array. The instrument takes limb images of the atmosphere from the flight altitude of HALO or M55-Geophysica down to 4 km with a vertical sampling step of about 150 m at 10 km tangent height. Individual images contain 128 pixels (spectra) in the vertical dimension and 48 pixels in the horizontal dimension. The spectral range of the observations currently extends from about 780 cm^{-1} to 1400 cm^{-1}. The list of measurable quantities includes temperature, H_2O, HDO, O_3, CH_4, N_2O, CFC-11, CFC-12, HCFC-12, SF_6, HNO_3, N_2O_5, $ClONO_2$, HO_2NO_2, PAN, C_2H_6, H_2CO, NH_3, and cirrus cloud quantities like effective radii and ice water content (IWC). Details on the instrument design and calibration are given in the accompanying publications of Friedl-Vallon et al. (2014) and Kleinert et al. (2014).

GLORIA is operated in a high-spectral, medium-spatial sampling ("chemistry") mode and a medium-spectral, high-spatial sampling ("dynamics") mode (see below). The spectral samplings are 0.065 cm^{-1} for the chemistry mode and 0.65 cm^{-1} for the dynamics mode, respectively. Other combinations of spectral and spatial resolution can be used, if desirable for a specific scientific objective. In the dynamics mode, the time saved by running the interferometer at a much shorter optical path difference (i.e. lower spectral resolution) is used for pannig the line-of-sight from about 45° to 135° with respect to the aircraft flight-direction. An illustration of the panning, which allows for tomographic applications, is given in the left panel of Fig. 4. The overlap of different viewing angles in the same air volume can be used for tomographic retrievals, also in the case of a linear flight pattern (left panel of Fig. 4). These tomographic capabilities can be even enhanced by chosing a closed flight pattern as illutrated in the right panel of Fig. 4 for a circle (Ungermann et al., 2010, 2011). The high spatial density of tangent points resulting from the large range of viewing angles in a closed-path tomography is illustrated in Fig. 5. First results of a tomographic measurement of a fine filament of enhanced HNO_3 values are presented in Sect. 3.2.

The GLORIA chemistry mode is optimized in terms of spectral instead of horizontal resolution. The high spectral sampling of about 0.065 cm^{-1} allows the retrieval of trace gases which cannot (or less reliably) be derived in the dynamics mode. The larger interferometer sweep time needed for one limb image at maximum spectral resolution results in a reduced along-track sampling while maintaining the same vertical sampling at a fixed azimuth angle. The chemistry mode is especially suited for the reconstruction of 2-D distributions (curtains) of a huge number of trace gases along the flight track rather than tomographically resolved 3-D temperature or trace gas fields. As an example, Fig. 6 shows measurements of ethane (C_2H_6) retrieved from chemistry mode measurements on 18 September 2012 for a flight between the Maledives and Zyprus. C_2H_6 is a typical tracer for polluted air, being produced by biomass burning and fossil fuel production with a tropospheric lifetime of few months (Xiao et al., 2008). The enhancements of C_2H_6 in Fig. 6 point to transport of polluted air into the free troposphere and the UTLS either from local source or large scale advection from the monsoon area.

3.2 First tomographic observations

The first tomographic observations took place during the TACTS and ESMVal aircraft campaign in summer/autumn 2012. Due to operational aircraft constraints, hexagons with a typical segment length of 200 km were chosen as closed paths instead of circles for enhanced tomographic applications. The high tangent point density resulted in a horizontal resolution of up to 20 km × 20 km for temperature structures and atmospheric trace species such as ozone, HNO_3, CFC-11, and water vapour (Blank, 2013).

Figure 7 shows the HALO flight pattern south of Capetown (Southern Africa) for 12 September 2012 during the ESMVal campaign. GLORIA encountered a situation with highly variable trace gas fields resulting from a planetary wave breaking event, which is indicated by a large northward diplacement of polar air at 12 km altitude. Polar vortex air can be identified by large absolute values of potential vorticity. The HALO flight track including the position of the tomographic hexagon and indications of tangent point locations is also shown in Fig. 7. GLORIA observations in the tomographic volume confirm that this wave breaking event was associated with pronounced small-scale trace gas filamentation. Figure 8 shows, in fact, the first three-dimensional tomographic observation of a small-scale filament of stratospheric air (enhanced HNO_3 values), which is surrounded by tropospheric air. A more detailed description of these tomographic measurements and quantitative retrieval results, including the achievable vertical and horizontal resolution and error estimates, is given in the accompanying publication of Kaufmann et al. (2014). GLORIA achieves a vertical resolution up to 300 m and a horizontal resolution down to 20 km × 20 km for temperature structures and a number of trace gases. This represents an important prerequisite for major contributions to the specific scientific questions outlined in Sect. 4.

4 Specific scientific objectives

4.1 Composition of the extra-tropical UTLS

In the extra-tropical UTLS, air is a mixture of aged air masses, which have been transported downward by the stratospheric (Brewer–Dobson) circulation through the deep stratosphere, and young air masses, which have been transported isentropically from low to high latitudes or convectively upward from the troposphere. An overview on the processes influencing the extra-tropical UTLS is given by Gettelman et al. (2011). Some of the important features are illustrated in Fig. 9. The composition of the extra-tropical lowermost stratosphere (LMS) is strongly influenced by isentropic (quasi-horizontal) transport of air masses from the tropics. This poleward transport is related to Rossby-wave breaking and reverses its seasonality at altitudes above 420 K (e.g., Homeyer and Bowman, 2013). Above 420 K, transport maximizes during winter and is related to structures from large-scale planetary tongues (streamers) to filaments of subtropical air that are mixed into the winter stratosphere (Randel et al., 1993; Riese et al., 1999b, 2002). Below 420 K, transport maximizes during summer and fall. Related intrusions of low latitude air may reach deep into mid and high latitudes (e.g., Pan et al., 2009; Vogel et al., 2011).

First observations during the HALO missions TACTS and ESMVal in summer/fall 2012 demonstrate the capability of GLORIA to resolve small-scale transport structures related to wave breaking events (Fig. 8). Dedicated studies of this transport are planned for the Wave-driven ISentropic Exchange (WISE) campaign (HALO) in autumn 2017. Major scientific objectves of WISE concern the relationship between the extra-tropical transition layer (ExTL) and the tropopause inversion layer (TIL), quasi-horizontal transport into the lowermost stratosphere (LMS) above the ExTL, the occurence of sub-visible cirrus clouds in the LMS, and the influence of the Asian Summer Monsoon on the water vapour budget in the extra-tropical LMS (see Sects. 4.1.1 to 4.1.3.). In addition, the composition of the extra-tropical UTLS may be significantly influenced by isentropic transport of polar air masses (and subsequent mixing) resulting from the springtime breakup of the polar vortex. Studies of this influence are in the centre of the Polar Stratosphere in a Changing Climate (POLSTRACC) campaign (HALO) in winter/spring 2015/2016.

4.1.1 Extra-tropical transition layer and tropopause inversion layer

The extra-tropical transition layer (ExTL), as illustrated in Fig. 9, is generated by bi-directional mixing across the tropopause (e.g., Fischer et al., 2000; Hoor et al., 2002; Krebsbach et al., 2006). The vertical depth of the ExTL is about 25 K in the LMS with respect to the local tropopause (Hoor et al., 2004). The layer is most pronounced during summer and exhibits large seasonal variability. The formation of the ExTL is a result of disturbances of the subtropical jet by large-scale wave activity (timescales of days to weeks) or transport from below, for example, by warm conveyor belts or deep convection (e.g., Anderson et al., 2012).

Analyses of airborne in-situ observations (Kunz et al., 2009) and satellite observations (Hegglin et al., 2009) suggest a relation between the ExTL and the dynamical feature of the tropopause inversion layer (TIL). The TIL represents a vertically narrow

AMTD
7, 1535–1572, 2014

region of strongly enhanced static stability directly above the extra-tropical tropopause (Birner et al., 2002, 2006; Wirth, 2003). Several mechanisms contributing to the formation of the TIL have been discussed such as effects of the residual circulation (Birner, 2010) or baroclinic wave breaking events in the extra-tropics (Son and Polvani, 2007). Randel et al. (2007) suggest a radiation-controlled formation and maintenance of the TIL, mainly involving water vapour and ozone.

The relative contributions of dynamics and radiation processes on the formation of the TIL is still a matter of debate. According to Kunz et al. (2009), a rather well-mixed ExTL appears to be a pre-requisite for a radiation-controlled formation of the TIL. It is, however, unclear to what extent the TIL, in turn, affects the spatial distribution of radiatively active species such as water vapour and ozone. The unique combination of GLORIA three-dimensional high-resolution observations of temperature, which can be converted to static stability (N^2), water vapour, ozone, and cirrus clouds is ideally suited to investigate this question. Moreover, GLORIA remote-sensing data will be complemented during WISE by a comprehensive set of in-situ observations, which provides detailed information on mixing processes based the tracer-tracer correlation technique and corresponding model simulations (e.g., Vogel et al., 2011).

4.1.2 Quasi-horizontal transport above the ExTL

The composition of the Northern Hemisphere LMS is strongly influenced Rossby-wave breaking, which occurs mainly over the Northern Atlantic and Pacific during summer and autumn (e.g., Postel and Hitchman, 1999; Homeyer and Bowman, 2013). Ploeger et al. (2013) showed that close to the subtropics, the isentropic (quasi horizontal) transport in the upper part of the LMS (around 400 K) is mainly caused by the residual circulation (shallow branch), while at middle to high latitudes large-scale eddy mixing dominates the horizontal water vapour transport. The dominant influence of frequent horizontal transport from subtropical latitudes extends up to about 450 K during summer and fall, and is reflected in a clear anti-correlation between water vapour and ozone in both Microwave Limb Sounder (MLS) observations (Livesey et al., 2006) and

AMTD
7, 1535–1572, 2014

GLORIA scientific objectives

M. Riese et al.

simulations by the Chemical Lagrangian Model of the Stratosphere (CLaMS). However, the study of Ploeger et al. (2013) also revealed significant differences between the observed and simulated anti-correlations that can be attributed to the finite resolution of the satellite observations and imperfections of the transport simulated by CLaMS. Envisaged GLORIA measurements during WISE are perfectly suited to test the capability of models like CLaMS to capture medium und small-scale transport structures (e. g. filaments) and associated anti-correlations between water vapour and ozone. Another important objective is the investigation of air masses with enhanced amounts of water vapour and pollutants in the LMS, originating from convective uplift by the Asian Monsoon (see Ploeger et al., 2013). Such air masses have been detected by in-situ measurements onboard HALO during TACTS and could be traced back to the Asian Monsoon by CLaMS simulations and trajectory calculations (Vogel et al., 2014).

4.1.3 Occurence of sub-visible cirrus clouds in the LMS

Transport of water vapour also plays an important role for the formation of cirrus clouds. Presently, the importance of various water vapour pathways into the LMS on sub-visible cirrus formation is controversially discussed (e.g., Dessler, 2009; Pan and Munchak, 2011). Ground based cloud observations from mid-latitude lidar stations show occasionally subvisible cirrus cloud events at and above the tropopause (Keckhut et al., 2005). Many of them coincide with observations of a secondary tropopause (Noel and Haeffelin, 2007). These events may be caused by isentropic water vapour transport from the sub-tropics associated with Rossby-wave breaking (e.g., Eixmann et al., 2010). Infrared limb observations of cirrus clouds during the CRISTA-2 mission in 1997 also suggest frequent cirrus events around the mid-latitude tropopause (Spang et al., 2002).

An important issue for the detection of sub-visible cirrus clouds is the sensor sensitivity. Passive nadir sounders substantially underestimate the occurrence of sub-visible cirrus clouds (SVCs) in comparison to IR limb sounders (e.g., Spang et al., 2012). Even active lidars are less sensitive and may underestimate the occurence frequency

AMTD
7, 1535–1572, 2014
GLORIA scientific objectives
M. Riese et al.

of SVCs. For example, the ice water content (IWC) threshold for CALIOP lidar nadir-observations is in the range of 0.1 to $4 \times 10^{-3}\,\mathrm{g\,m^{-3}}$, while IWCs of about $10^{-6}\,\mathrm{g\,m^{-3}}$ are detectable by infrared limb-viewing for a cirrus cloud layer with a horizontal extent of about 30 km (or larger) (Spang et al., 2012). The high sensitivity of IR limb sounding with respect to vertically very thin cloud layers was already demonstrated by Spang et al. (2008) based on CRISTA-NF observations. GLORIA provides both high sensitivity and a unique view on the three-dimensional structure of sub-visible cirrus including their position with respect to the thermal tropopause. Measurements during WISE will cover the north Atlantic to Scandinavia region, which is a preferential region for sub-visible cirrus clouds in the LMS (Spang et al., 2014). The high occurence rate in this region is a result of enhanced Rossby-wave activity (see above) and the occurrence of warm conveyor belts, which appear to trigger cirrus cloud formation in the upper troposphere (Spichtinger et al., 2005).

4.1.4 Influence of the Asian Summer Monsoon on UTLS composition

The Asian Monsoon circulation provides an important pathway for air masses from the troposphere into the upper tropical troposphere and tropical tropopause layer (TTL). This transport influences the composition of the ascending branch of the Brewer–Dobson (BD) circulation in the lower stratosphere (Randel et al., 2010) as well as isentropic (quasi-horizontal) transport of water vapour and tropospheric pollutants from the tropics into the extra-tropical LMS (Ploeger et al., 2013).

An important part of the Asian Monsoon circulation is an anticyclone in the UT extending from Asia to the Middle East (Park et al., 2007). This anticyclone confines a region of persistent enhanced pollution caused by rapid vertical transport of polluted air from e.g. South China, India, and Indonesia by deep convection. Along the eastern flank of the monsoon anticyclone, air masses are transported equatorwards, affecting trace gas budgets in the TTL (e.g. heads of tape recorders), which are subsequently further lifted up by the BD circulation (Konopka et al., 2009, 2010; Ploeger et al., 2012). Along the western flank of the Asian Monsoon anticyclone, air is transported

AMTD
7, 1535–1572, 2014

into the extra-tropical LMS (Ploeger et al., 2013). An illustration of associated transport structures is given in Fig. 10 based on ozone concentrations simulated by CLaMS. Quantitative analyses of the associated transport and mixing processes require two- and three-dimensional observations of multiple trace gases with the highest achievable resolution, complemented by detailed (1-D) in-situ observations. GLORIA will provide such observations onboard M55-Geophysica during the Stratospheric and upper tropospheric processes for better Climate predictions (StratoClim) tropical aircraft campaign (FP7) in summer 2015.

4.2 Evolution of the polar stratosphere in a changing climate

The polar stratosphere is important for the evolution of the global ozone layer and the climate system. While the amounts of ozone depleting substances in the stratosphere are expected to decrease in the next decades due to the restrictions following the Montreal protocol, colder Arctic temperatures may result in a more frequent appearance of polar stratospheric clouds (PSCs), extended ozone depletion and a delay in global ozone recovery (e.g., Sinnhuber et al., 2011). Furthermore, chemically processed air from the polar vortex can enter the mid-latitude LMS via fast transport processes and can affect the local chemical composition and radiation budget (e.g., Werner et al., 2010). A detailed understanding of these processes is necessary to allow reliable estimations for the evolution of the ozone layer and the role of the polar stratosphere in the future climate.

Previous studies utilizing the balloon-borne MIPAS-instrument have shown that accurate observations of the budgets of NO_y and chlorine species (e.g., Wiegele et al., 2009; Wetzel et al., 2010) as well as important photochemical processes (Wetzel et al., 2012) are possible using infrared limb observations. Measurements by MIPAS-STR and CRISTA-NF have shown that vortex filaments and extra vortex air can be identified using this technique (e.g., Ungermann et al., 2012; Woiwode et al., 2012) and allow for detailed studies of stratospheric dynamics in combination with high-resolution chemistry transport modelling (Kalicinsky et al., 2013). During the HALO campaign

AMTD
7, 1535–1572, 2014

POLSTRACC in the Arctic winter/spring 2015/16, GLORIA will provide spatially highly resolved observations allowing detailed investigations of key processes such as NO_y redistribution following denitrification, PSC occurrence and composition, and chlorine activation and de-activaton. Furthermore, the measurements will allow to study transport processes between vortex and extra vortex air as well as between the LMS and the UT. Chemical and dynamical processes under the present load of halogens and the state of climate variables in the middle of the 2010s will be studied in contrast to what was present 10 to 20 yr ago.

4.3 Gravity wave observations

The atmosphere impacts on surface climate via radiative and dynamical processes. In particular, there is growing evidence that dynamical couplings in the stratosphere-troposphere system have a significant impact on regional weather patterns and climate, mainly through changes of the Northern and Southern Hemisphere Annular Modes (NAM and SAM, respectively). Predicted changes of the strength of the stratospheric BD circulation may also modify tropospheric weather patterns. Small-scale gravity waves (GWs) play an important role in these atmospheric couplings but also represent a major source of uncertainty (Sigmond and Scinocca, 2010). Parameterized gravity wave drag may also account for much of the potential future trend of the Brewer–Dobson circulation in atmospheric models (e.g., McLandress and Shepherd, 2009; Butchart et al., 2010). However, these effects are far from being well understood. The largest uncertainties in atmospheric wave dynamics are associated with gravity waves, their sources, their propagation, and the representation of their characteristics in global models (Alexander et al., 2010).

The great potential of infrared limb-sounding to provide valuable information on gravity waves has been demonstrated in several studies (e.g. Fetzer and Gille, 1994; Eckermann and Preusse, 1999; Ern et al., 2006, 2011; Preusse et al., 2009; Geller et al., 2013). High-resolution 3-D temperature observations (300 m × 30 km × 30 km) by GLORIA will allow for simultaneous determination of gravity-wave temperature

AMTD
7, 1535–1572, 2014

amplitudes and associated horizontal and vertical wavelength (wave-vector) down to the mesoscale. From these quantities direction-resolved momentum-flux can be derived and gravity-waves can be traced back to their sources. This appoach will provide important constraints for gravity wave models and parametrisations. Corresponding observations are planned for the HALO campaign Gravity Wave Life Cycle (GW-LCycle), which is combined with POLSTRACC and will take place in winter/spring 2015/16.

5 Conclusions

In the past, infrared limb-sounding provided a wealth of data for investigations of the composition and dynamic structure of the middle atmosphere, in particular on the large scale. A new focus is the region of the upper troposphere/lower stratosphere (UTLS), which plays a crucial role in the climate system. Currently, there is an observational gap between synoptic-scale composition structures resolved by satellites and small-scale variability resolved by airborne in-situ instruments. Filling this gap is essential, because small- and meso-scale physical and chemical processes (trace gas exchange, clouds, gravity waves) play a crucial role for the composition and dynamic structure of the UTLS.

The Gimballed Limb Observer for Radiance Imaging (GLORIA) instrument addresses the observational gap in the UTLS by providing two- and three-dimensional observations of temperature structures, trace gases, and subvisible cirrus clouds with unprecedented spatial resolution. The vertical resolution of the observations is up to 300 m for both dynamics and chemistry mode. Novel tomographic observations provide a horizontal resolution down to 20 km × 20 km for temperature structures and most of the observable trace species. GLORIA therefore provides adequate spatial resolution for improved process studies in the UTLS.

Important scientific questions for GLORIA concern the interaction of the extra-tropical transition layer (ExTL) with the Tropopause Inversion Layer (TIL) as well as isentropic (quasi-horizontal) exchange of air masses between the tropical UT and the

AMTD
7, 1535–1572, 2014

extra-tropical LMS. The influence of isentropic water vapour transport from the tropics on the occurence of subvisible cirrus clouds in the LMS can be investigated on the basis of GLORIA's high sensitivity to optically thin subvisible cirrus clouds. Furthermore, the GLORIA measurements will allow to study ozone and climate-relevant processes in the Arctic UTLS as well as exchange processes between vortex and extra vortex air and between the LMS and UT in detail. Besides composition measurements, GLORIA will also enhance our knowledge on gravity-wave processes by providing direction-resolved momentum flux, and thus, deliver important constraints for gravity wave representations in global models.

Acknowledgements. We thank all members of the GLORIA instrument team for their large efforts in developing the first IR limb-imager. The GLORIA hardware was mainly funded by the Helmholtz Association of German Reserach Centres through several large investment funds. The development of the retrieval algorithms was supported by the Deutsche Forschungsgemeinschaft through the RASSGLO project. We also wish to thank Lars Hoffmann, who developed the JURASSIC-1 forward model and significantly contributed to several ESA studies of the limb-imaging concept. Many scientist involved in TACTS, ESMVal, POLSTRACC, GW-LCycle, and WISE contributed to fruitful discussions of the GLORIA science objectives. We thank the CLaMS team for assisting the flight planning by CLaMS model forecasts supported by German Research Foundation (DFG) under the project LASSO (HALO-SPP 1294/GR 3786). The operational implementation of the first tomographic flights was supported by Harald Bönsich and Andreas Engel, who coordinated TACTS. We also gratefully acknowledge the funding of the ESMVal flight hours by DLR and the coordination of ESMVal by Hans Schlager.

The service charges for this open access publication have been covered by a Research Centre of the Helmholtz Association.

References

Alexander, M. J., Geller, M., McLandress, C., Polavarapu, S., Preusse, P., Sassi, F., Sato, K., Eckermann, S., Ern, M., Hertzog, A., Kawatani, Y., Pulido, M., Shaw, T. A., Sigmond, M., Vin-

AMTD
7, 1535–1572, 2014
GLORIA scientific objectives
M. Riese et al.

cent, R., and Watanabe, S.: Recent developments in gravity-wave effects in climate models and the global distribution of gravity-wave momentum flux from observations and models, Q. J. Roy. Meteorol. Soc., 136, 1103–1124, doi:10.1002/qj.637, 2010. 1549

Anderson, J. G., Wilmouth, D. M., Smith, J. B., and Sayres, D. S.: UV dosage levels in summer: increased risk of ozone loss from convectively injected water vapor, Science, 337, 835–839, doi:10.1126/science.1222978, 2012. 1544

Bingham, G. E., Zhou, D. K., Bartschi, B. Y., Anderson, G. P., Smith, D. R., Chetwynd, J. H., and Nadile, R. M.: Cryogenic Infrared Radiance Instrumentation for Shuttle (CIRRIS 1A) Earth limb spectral measurements, calibration, and atmospheric O_3, HNO_3, CFC-12, and CFC-11 profile retrieval, J. Geophys. Res.-Atmos., 102, 3547–3558, 1997. 1538

Birner, T.: Residual circulation and tropopause structure, J. Atmos. Sci., 67, 2582–2600, doi:10.1175/2010JAS3287.1, 2010. 1545

Birner, T., Dörnbrack, A., and Schumann, U.: How sharp is the tropopause at midlatitudes?, Geophys. Res. Lett., 29, 1700, doi:10.129/2002GL015142, 2002. 1545

Birner, T., Sankey, D., and Shepherd, T. G.: The tropopause inversion layer in models and analyses, Geophys. Res. Lett., 33, L14808, doi:10.1029/2006GL026549, 2006. 1545

Blank, J.: Tomographic retrieval of atmospheric trace gases observed by GLORIA, Dissertation, Universität Wuppertal, 2013. 1542

Butchart, N., Cionni, I., Eyring, V., Shepherd, T. G., Waugh, D. W., Akiyoshi, H., Austin, J., Bruehl, C., Chipperfield, M. P., Cordero, E., Dameris, M., Deckert, R., Dhomse, S., Frith, S. M., Garcia, R. R., Gettelman, A., Giorgetta, M. A., Kinnison, D. E., Li, F., Mancini, E., McLandress, C., Pawson, S., Pitari, G., Plummer, D. A., Rozanov, E., Sassi, F., Scinocca, J. F., Shibata, K., Steil, B., and Tian, W.: Chemistry-climate model simulations of twenty-first century stratospheric climate and circulation changes, J. Climate, 23, 5349–5374, doi:10.1175/2010JCLI3404.1, 2010. 1549

Dessler, A. E.: Clouds and water vapor in the Northern Hemisphere summertime stratosphere, J. Geophys. Res.-Atmos., 114, D00H9, doi:10.1029/2009JD012075, 2009. 1546

Drummond, J. R., Houghton, J. T., Peskett, G. D., Rodgers, C. D., Wale, M. J., Whitney, J., and Williamson, E. J.: The stratospheric and mesospheric sounder on Nimbus 7, Philos. T. R. Soc. S.-A, 296, 219–241, doi:10.1098/rsta.1980.0166, 1980. 1538

Eckermann, S. D. and Preusse, P.: Global measurements of stratospheric mountain waves from space, Science, 286, 1534–1537, 1999. 1549

AMTD

7, 1535–1572, 2014

GLORIA scientific objectives

M. Riese et al.

Eixmann, R., Peters, D. H. W., Zuelicke, C., Gerding, M., and Doernbrack, A.: On the upper tropospheric formation and occurrence of high and thin cirrus clouds during anticyclonic poleward Rossby wave breaking events, Tellus, 62, 228–242, doi:10.1111/j.1600-0870.2010.00437.x, 2010. 1546

Ern, M., Preusse, P., and Warner, C. D.: Some experimental constraints for spectral parameters used in the Warner and McIntyre gravity wave parameterization scheme, Atmos. Chem. Phys., 6, 4361–4381, doi:10.5194/acp-6-4361-2006, 2006. 1549

Ern, M., Preusse, P., Gille, J. C., Hepplewhite, C. L., Mlynczak, M. G., Russell, III, J. M., and Riese, M.: Implications for atmospheric dynamics derived from global observations of gravity wave momentum flux in stratosphere and mesosphere, J. Geophys. Res.-Atmos., 116, D19107, doi:10.1029/2011JD015821, 2011. 1549

ESA: Report for Mission Selection: PREMIER, vol. SP-1324/3, ESA Communication Production Office, Noordwijk, the Netherlands, 2012. 1539

Fetzer, E. J. and Gille, J. C.: Gravity wave variance in LIMS temperatures, Part I: Variability and comparison with background winds, J. Atmos. Sci., 51, 2461–2483, 1994. 1549

Fischer, H. and Oelhaf, H.: Remote sensing of vertical profiles of atmospheric trace constituents with MIPAS limb-emission spectrometers, Appl. Optics, 35, 2787–2796, 1996. 1539

Fischer, H., Wienhold, F., Hoor, P., Bujok, O., Schiller, C., Siegmund, P., Ambaum, M., Scheeren, H., and Lelieveld, J.: Tracer correlations in the northern high latitude lowermost stratosphere: influence of cross-tropopause mass exchange, Geophys. Res. Lett., 27, 97–100, doi:10.1029/1999GL010879, 2000. 1544

Fischer, H., Birk, M., Blom, C., Carli, B., Carlotti, M., von Clarmann, T., Delbouille, L., Dudhia, A., Ehhalt, D., Endemann, M., Flaud, J. M., Gessner, R., Kleinert, A., Koopman, R., Langen, J., López-Puertas, M., Mosner, P., Nett, H., Oelhaf, H., Perron, G., Remedios, J., Ridolfi, M., Stiller, G., and Zander, R.: MIPAS: an instrument for atmospheric and climate research, Atmos. Chem. Phys., 8, 2151–2188, doi:10.5194/acp-8-2151-2008, 2008. 1537, 1538, 1539

Friedl-Vallon, F., Maucher, G., Seefeldner, M., Trieschmann, O., Kleinert, A., Lengel, A., Keim, C., Oelhaf, H., and Fischer, H.: Design and characterization of the balloon-borne michelson interferometer for passive atmospheric sounding (MIPAS-B2), Appl. Optics, 43, 3335–3355, doi:10.1364/AO.43.003335, 2004. 1539

Discussion Paper | Discussion Paper | Discussion Paper | Discussion Paper |

AMTD

7, 1535–1572, 2014

GLORIA scientific objectives

M. Riese et al.

Friedl-Vallon, F., Riese, M., Maucher, G., Lengel, A., Hase, F., Preusse, P., and Spang, R.: Instrument concept and preliminary performance analysis of GLORIA, Adv. Space Res., 37, 2287–2291, doi:10.1016/j.asr.2005.07.075, 2006. 1539

Friedl-Vallon, F., Gulde, T., Hase, F., Kleinert, A., Kulessa, T., Maucher, G., Neubert, T., Olschewski, F., Piesch, C., Preusse, P., Rongen, H., Sartorius, C., Schneider, H., Schönfeld, A., Tan, V., Bayer, N., Blank, J., Dapp, R., Ebersoldt, A., Fischer, H., Guggenmoser, T., Höpfner, M., Kaufmann, M., Kretschmer, E., Nordmeyer, H., Oelhaf, H., Orphal, J., Riese, M., Schardt, G., Schillings, J., Sha, M. K., Suminska-Ebersoldt, O., and Ungermann, J.: Instrument concept of the imaging Fourier transform spectrometer GLORIA, Atmos. Meas. Tech. Discuss., in preparation, 2014.

Geller, M. A., Alexander, M. J., Love, P. T., Bacmeister, J., Ern, M., Hertzog, A., Manzini, E., Preusse, P., Sato, K., Scaife, A. A., and Zhou, T.: A comparison between gravity wave momentum fluxes in observations and climate models, J. Climate, 26, 6383–6405, doi:10.1175/JCLI-D-12-00545.1, 2013. 1549

Gettelman, A., Hoor, P., Pan, L. L., Randel, W. J., Hegglin, M. I., and Birner, T.: The extra tropical upper troposphere and lower stratosphere, Rev. Geophys., 49, RG3003, doi:10.1029/2011RG000355, 2011. 1543

Gille, J. C. and Russel III, J. M.: The Limb Infrared Monitor of the stratosphere: experiment description, performance, and results, J. Geophys. Res.-Atmos., 89, 5125–5140, doi:10.1029/JD089iD04p05125, 1984. 1538

Gille, J. C., Barnett, J., Arter, P., Barker, M., Bernath, P., Boone, C., Cavanaugh, C., Chow, J., Coffey, M., Craft, J., Craig, C., Dials, M., Dean, V., Eden, T., Edwards, D. P., Francis, G., Halvorson, C., Harvey, L., Hepplewhite, C., Khosravi, R., Kinnison, D., Krinsky, C., Lambert, A., Lee, H., Lyjak, L., Loh, J., Mankin, W., Massie, S., McInerney, J., Moorhouse, J., Nardi, B., Packman, D., Randall, C., Reburn, J., Rudolf, W., Schwartz, M., Serafin, J., Stone, K., Torpy, B., Walker, K., Waterfall, A., Watkins, R., Whitney, J., Woodard, D., and Young, G.: The high-resolution dynamics limb sounder: experiment overview, recovery, and validation of initial temperature data, J. Geophys. Res.-Atmos., 113, D16S43, doi:10.1029/2007JD008824, 2008. 1538

Grossmann, K. U., Offermann, D., Gusev, O., Oberheide, J., Riese, M., and Spang, R.: The CRISTA-2 mission, J. Geophys. Res.-Atmos., 107, D23, doi:10.1029/2001JD000667, 2002. 1538

AMTD
7, 1535–1572, 2014
GLORIA scientific objectives
M. Riese et al.

Hegglin, M. I., Boone, C. D., Manney, G. L., and Walker, K. A.: A global view of the extratropical tropopause transition layer from Atmospheric Chemistry Experiment Fourier Transform Spectrometer O_3, H_2O, and CO, J. Geophys. Res.-Atmos., 114, D00B11, doi:10.1029/2008JD009984, 2009. 1544

Hoffmann, L., Weigel, K., Spang, R., Schroeder, S., Arndt, K., Lehmann, C., Kaufmann, M., Ern, M., Preusse, P., Stroh, F., and Riese, M.: CRISTA-NF measurements of water vapor during the SCOUT-O_3 Tropical Aircraft Campaign, Adv. Space Res., 43, 74–81, doi:10.1016/j.asr.2008.03.018, 2009. 1540

Homeyer, C. R. and Bowman, K. P.: Rossby wave breaking and transport between the tropics and extratropics above the subtropical jet, J. Atmos. Sci., 70, 607–626, doi:10.1175/JAS-D-12-0198.1, 2013. 1543, 1545

Hoor, P., Fischer, H., Lange, L., Lelieveld, J., and Brunner, D.: Seasonal variations of a mixing layer in the lowermost stratosphere as identified by the CO–O_3 correlation from in situ measurements, J. Geophys. Res.-Atmos., 107, 4004, doi:10.1029/2000JD000289, 2002. 1544

Hoor, P., Gurk, C., Brunner, D., Hegglin, M. I., Wernli, H., and Fischer, H.: Seasonality and extent of extratropical TST derived from in-situ CO measurements during SPURT, Atmos. Chem. Phys., 4, 1427–1442, doi:10.5194/acp-4-1427-2004, 2004. 1544

Kalicinsky, C., Grooß, J.-U., Günther, G., Ungermann, J., Blank, J., Höfer, S., Hoffmann, L., Knieling, P., Olschewski, F., Spang, R., Stroh, F., and Riese, M.: Observations of filamentary structures near the vortex edge in the Arctic winter lower stratosphere, Atmos. Chem. Phys., 13, 10859–10871, doi:10.5194/acp-13-10859-2013, 2013. 1540, 1548

Kaufmann, M., Blank, J., Guggenmoser, T., Ungermann, J., Engel, A., Ern, M., Friedl-Vallon, F., Gerber, D., Guenther, J. U. G., Höpfner, M., Kleinert, A., Latzko, Th., Maucher, G., Neubert, T., Nordmeyer, H., Oelhaf, H., Olschewski, F., Orphal, J., Preusse, P., Schlager, H., Schneider, H., Schüttemeyer, D., Stroh, F., Suminska-Ebersoldt, O., Vogel, B., Volk, C. M., Woiwode, W., and Riese, M.: Retrieval of three-dimensional small scale structures in upper tropospheric/lower stratospheric composition as measured by GLORIA, Atmos. Meas. Tech. Discuss., in preparation, 2014.

Keckhut, P., Hauchecorne, A., Bekki, S., Colette, A., David, C., and Jumelet, J.: Indications of thin cirrus clouds in the stratosphere at mid-latitudes, Atmos. Chem. Phys., 5, 3407–3414, doi:10.5194/acp-5-3407-2005, 2005. 1546

Keim, C., Liu, G. Y., Blom, C. E., Fischer, H., Gulde, T., Höpfner, M., Piesch, C., Ravegnani, F., Roiger, A., Schlager, H., and Sitnikov, N.: Vertical profile of peroxyacetyl nitrate (PAN) from

MIPAS-STR measurements over Brazil in February 2005 and its contribution to tropical UT NO_y partitioning, Atmos. Chem. Phys., 8, 4891–4902, doi:10.5194/acp-8-4891-2008, 2008. 1540

Kleinert, A., Friedl-Vallon, F., Guggenmoser, T., Höpfner, M., Neubert, T., Ribalda, R., Sha, M. K., Ungermann, J., Blank, J., Ebersoldt, A., Kretschmer, E., Latzko, T., Oelhaf, H., Olschewski, F., and Preusse, P.: Level 0 to 1 processing of the imaging Fourier transform spectrometer GLORIA: Generation of radiometrically and spectrally calibrated spectra, Atmos. Meas. Tech. Discuss., in preparation, 2014.

Konopka, P., Grooß, J.-U., Plöger, F., and Müller, R.: Annual cycle of horizontal in-mixing into the lower tropical stratosphere, J. Geophys. Res.-Atmos., 114, 148–227, doi:10.1029/2009JD011955, 2009. 1547

Konopka, P., Grooß, J.-U., Günther, G., Ploeger, F., Pommrich, R., Müller, R., and Livesey, N.: Annual cycle of ozone at and above the tropical tropopause: observations versus simulations with the Chemical Lagrangian Model of the Stratosphere (CLaMS), Atmos. Chem. Phys., 10, 121–132, doi:10.5194/acp-10-121-2010, 2010. 1547

Krebsbach, M., Schiller, C., Brunner, D., Günther, G., Hegglin, M. I., Mottaghy, D., Riese, M., Spelten, N., and Wernli, H.: Seasonal cycles and variability of O_3 and H_2O in the UT/LMS during SPURT, Atmos. Chem. Phys., 6, 109–125, doi:10.5194/acp-6-109-2006, 2006. 1544

Kullmann, A., Riese, M., Olschewski, F., Stroh, F., and Grossmann, K. U.: Cryogenic Infrared Spectrometers and Telescopes for the Atmosphere – New Frontiers, in: Proc. SPIE, vol. 5570, 423–432, doi:10.1117/12.564856, 2004. 1538

Kunz, A., Konopka, P., Müller, R., Pan, L. L., Schiller, C., and Rohrer, F.: High static stability in the mixing layer above the extratropical tropopause, J. Geophys. Res.-Atmos., 114, D16305, doi:10.1029/2009JD011840, 2009. 1544, 1545

Livesey, N., Van Snyder, W., Read, W., and Wagner, P.: Retrieval algorithms for the EOS Microwave limb sounder (MLS), IEEE T. Geosci. Remote, 44, 1144–1155, doi:10.1109/TGRS.2006.872327, 2006. 1545

Lorenz, E. N.: Deterministic non-periodic flow, J. Atmos. Sci., 20, 130–141, 1963. 1537

McLandress, C. and Shepherd, T. G.: Simulated anthropogenic changes in the Brewer–Dobson circulation, including its extension to high latitudes, J. Climate, 22, 1516–1540, doi:10.1175/2008JCLI2679.1, 2009. 1549

Noel, V. and Haeffelin, M.: Midlatitude cirrus clouds and multiple tropopauses from a 2002–2006 climatology over the SIRTA observatory, J. Geophys. Res.-Atmos., 112, D13206, doi:10.1029/2006JD007753, 2007. 1546

Offermann, D., Grossmann, K.-U., Barthol, P., Knieling, P., Riese, M., and Trant, R.: Cryogenic Infrared Spectrometers and Telescopes for the Atmosphere (CRISTA) experiment and middle atmosphere variability, J. Geophys. Res.-Atmos., 104, 16311–16325, doi:10.1029/1998JD100047, 1999. 1538

Pan, L. L. and Munchak, L. A.: Relationship of cloud top to the tropopause and jet structure from CALIPSO data, J. Geophys. Res.-Atmos., 116, D12201, doi:10.1029/2010JD015462, 2011. 1546

Pan, L. L., Randel, W. J., Gille, J. C., Hall, W. D., Nardi, B., Massie, S., Yudin, V., Khosravi, R., Konopka, P., and Tarasick, D.: Tropospheric intrusions associated with the secondary tropopause, J. Geophys. Res.-Atmos., 114, D10302, doi:10.1029/2008JD011374, 2009. 1544

Park, M., Randel, W. J., Gettelman, A., Massie, S. T., and Jiang, J. H.: Transport above the Asian summer monsoon anticyclone inferred from Aura Microwave Limb Sounder tracers, J. Geophys. Res.-Atmos., 112, D16309, doi:10.1029/2006JD008294, 2007. 1547

Piesch, C., Gulde, T., Sartorius, C., Friedl-Vallon, F., Seefeldner, M., Wölfel, M., Blom, C., and Fischer, H.: Design of a MIPAS Instrument for High-Altitude Aircraft, in: Proc. of the Second Internat. Airborne Remote Sensing Conference and Exhibition, vol. II, Ann Arbor, MI, 199–208, 1996. 1539

Ploeger, F., Konopka, P., Müller, R., Fueglistaler, S., Schmidt, T., Manners, J. C., Grooss, J.-U., Günther, G., Forster, P. M., and Riese, M.: Horizontal transport affecting trace gas seasonality in the Tropical Tropopause Layer (TTL), J. Geophys. Res.-Atmos., 117, D09303, doi:10.1029/2011JD017267, 2012. 1547

Ploeger, F., Günther, G., Konopka, P., Fueglistaler, S., Müller, R., Hoppe, C., Kunz, A., Spang, R., Grooss, J. U., and Riese, M.: Horizontal water vapor transport in the lower stratosphere from subtropics to high latitudes during boreal summer, J. Geophys. Res.-Atmos., 118, 8111–8127, doi:10.1002/jgrd.50636, 2013. 1545, 1546, 1547, 1548

Postel, G. A. and Hitchman, M. H.: A climatology of Rossby wave breaking along the subtropical tropopause, J. Atmos. Sci., 56, 359–373, doi:10.1175/1520-0469(1999)056<0359:ACORWB>2.0.CO;2, 1999. 1545

Preusse, P., Schroeder, S., Hoffmann, L., Ern, M., Friedl-Vallon, F., Ungermann, J., Oelhaf, H., Fischer, H., and Riese, M.: New perspectives on gravity wave remote sensing by spaceborne infrared limb imaging, Atmos. Meas. Tech., 2, 299–311, doi:10.5194/amt-2-299-2009, 2009. 1549

Randel, W. J., Gille, J. C., Roche, A. E., Kumer, J. B., Mergenthaler, J. L., Waters, J. W., Fishbein, E. F., and Lahoz, W. A.: Stratospheric transport from the tropics to middle latitudes by planetary-wave mixing, Nature, 365, 533–535, 1993. 1543

Randel, W. J., Wu, F., and Forster, P.: The extratropical tropopause inversion layer: global observations with GPS data, and a radiative forcing mechanism, J. Atmos. Sci., 64, 4489–4496, doi:10.1175/2007JAS2412.1, 2007. 1545

Randel, W. J., Park, M., Emmons, L., Kinnison, D., Bernath, P., Walker, K. A., Boone, C., and Pumphrey, H.: Asian monsoon transport of pollution to the stratosphere, Science, 328, 611–613, doi:10.1126/science.1182274, 2010. 1547

Riese, M., Preusse, P., Spang, R., Ern, M., Jarisch, M., Grossmann, U., and Offermann, D.: Measurements of trace gases by the cryogenic infrared spectrometers and telescopes for the atmosphere CRISTA experiment, Adv. Space Res., 19, 563–566, doi:10.1016/S0273-1177(97)00172-5, 1997. 1538

Riese, M., Spang, R., Preusse, P., Ern, M., Jarisch, M., Offermann, D., and Grossmann, K. U.: Cryogenic Infrared Spectrometers and Telescopes for the Atmosphere (CRISTA) data processing and atmospheric temperature and trace gas retrieval, J. Geophys. Res.-Atmos., 104, 16349–16367, doi:10.1016/S0273-1177(97)00172-5, 1999a. 1538

Riese, M., Tie, X., Brasseur, G., and Offermann, D.: Three-dimensional simulation of stratospheric trace gas distributions measured by CRISTA, J. Geophys. Res.-Atmos., 104, 16419–16435, doi:10.1029/1999JD900178, 1999b. 1543

Riese, M., Manney, G. L., Oberheide, J., Tie, X., Spang, R., and Küll, V.: Stratospheric transport by planetary wave mixing as observed during CRISTA-2, J. Geophys. Res.-Atmos., 107, 8179, doi:10.1029/2001JD000629, 2002. 1543

Riese, M., Friedl-Vallon, F., Spang, R., Preusse, P., Schiller, C., Hoffmann, L., Konopka, P., Oelhaf, H., von Clarmann, T., and Höpfner, M.: GLObal limb Radiance Imager for the Atmosphere (GLORIA): scientific objectives, Adv. Space Res., 36, 989–995, doi:10.1016/j.asr.2005.04.115, 2005. 1539

Riese, M., Ploeger, F., Rap, A., Vogel, B., Konopka, P., Dameris, M., and Forster, P.: Impact of uncertainties in atmospheric mixing on simulated UTLS composition and related radiative

AMTD
7, 1535–1572, 2014
GLORIA scientific objectives
M. Riese et al.

effects, J. Geophys. Res.-Atmos., 117, D16305, doi:10.1029/2012JD017751, 2012. 1537, 1564
Roche, A. E., Kumer, J. B., Mergenthaler, J. L., Ely, G. A., Uplinger, W. G., Potter, J. F., James, T. C., and Sterritt, L. W.: The Cryogenic Limb Array Etalon Spectrometer (CLAES) on UARS: experiment description and performance, J. Geophys. Res.-Atmos., 98, 10763–10775, 1993. 1538
Russell, J. M., Mlynczak, M. G., Gordley, L. L., Tansock, J., and Esplin, R.: An overview of the SABER experiment and preliminary calibration results, in: Proc. SPIE, vol. 3756, 277–288, 1999. 1538
Sigmond, M., and Scinocca, J. F.: The influence of the basic state on the Northern Hemisphere circulation response to climate change, J. Climate, 23, 1434–1446, doi:10.1175/2009JCLI3167.1, 2010. 1549
Sinnhuber, B. M., Stiller, G., Ruhnke, R., von Clarmann, T., Kellmann, S., and Aschmann, J.: Arctic winter 2010/2011 at the brink of an ozone hole, Geophys. Res. Lett., 38, L24812, doi:10.1029/2011GL049784, 2011. 1548
Solomon, S., Qin, D., Manning, M., Alley, R., Berntsen, T., Bindoff, N., Chen, Z., Chidthaisong, A., Gregory, J., Hegerl, G., Heimann, M., Hewitson, B., Hoskins, B., Joos, F., Jouzel, J., Kattsov, V., Lohmann, U., Matsuno, T., Molina, M., Nicholls, N., J.Overpeck, Raga, G., Ramaswamy, V., Ren, J., Rusticucci, M., Somerville, R., Stocker, T., Whetton, P., Wood, R. A., and Wratt, D.: Climate Change 2007 – the Physical Science Basis, Contribution of Working Group I to the Fourth Assessment Report of the Intergovernmental Panel on Climate Change, chap. Technical Summary, Cambridge University Press, Cambridge, UK and New York, NY, USA, 2007. 1536
Solomon, S., Rosenlof, K. H., Portmann, R. W., Daniel, J. S., Davis, S. M., Sanford, T. J., and Plattner, G.-K.: Contributions of stratospheric water vapor to decadal changes in the rate of global warming, Science, 327, 1219–1223, doi:10.1126/science.1182488, 2010. 1536
Son, S.-W. and Polvani, L. M.: Dynamical formation of an extra-tropical tropopause inversion layer in a relatively simple general circulation model, Geophys. Res. Lett., 34, L17806, doi:10.1029/2007GL030564, 2007. 1545
Spang, R., Eidmann, G., Riese, M., Offermann, D., Preusse, P., Pfister, L., and Wang, P.-H.: CRISTA observations of cirrus clouds around the tropopause, J. Geophys. Res.-Atmos., 107, 8174, doi:10.1029/2001JD000698, 2002. 1546

AMTD
7, 1535–1572, 2014

Spang, R., Hoffmann, L., Kullmann, A., Olschewski, F., Preusse, P., Knieling, P., Schroeder, S., Stroh, F., Weigel, K., and Riese, M.: High resolution limb observations of clouds by the CRISTA-NF experiment during the SCOUT-O3 tropical aircraft campaign, Adv. Space Res., 42, 1765–1775, doi:10.1016/j.asr.2007.09.036, 2008. 1540, 1547

Spang, R., Arndt, K., Dudhia, A., Höpfner, M., Hoffmann, L., Hurley, J., Grainger, R. G., Griessbach, S., Poulsen, C., Remedios, J. J., Riese, M., Sembhi, H., Siddans, R., Waterfall, A., and Zehner, C.: Fast cloud parameter retrievals of MIPAS/Envisat, Atmos. Chem. Phys., 12, 7135–7164, doi:10.5194/acp-12-7135-2012, 2012. 1546, 1547

Spang, R., Günther, G., Riese, M., Hoffmann, L., Müller, R., and Griessbach, S.: Satellite observations and Lagrangian model study of cirrus clouds in the lowermost stratosphere, Atmos. Chem. Phys. Discuss., in preparation, 2014.

Spichtinger, P., Gierens, K., and Wernli, H.: A case study on the formation and evolution of ice supersaturation in the vicinity of a warm conveyor belt's outflow region, Atmos. Chem. Phys., 5, 973–987, doi:10.5194/acp-5-973-2005, 2005. 1547

Taylor, F., Rodgers, C., Whitney, J., Werrett, S., Barnett, J., Peskett, G., Venters, P., Ballard, J., Palmer, C., Knight, R., Morris, P., Nightingale, T., and Dudhia, A.: Remote-sensing of atmospheric structure and composition by pressure modulator radiometry from space – the ISAMS experiment on UARS, J. Geophys. Res.-Atmos., 98, 10799–10814, doi:10.1029/92JD03029, 1993. 1538

Ungermann, J., Kaufmann, M., Hoffmann, L., Preusse, P., Oelhaf, H., Friedl-Vallon, F., and Riese, M.: Towards a 3-D tomographic retrieval for the air-borne limb-imager GLORIA, Atmos. Meas. Tech., 3, 1647–1665, doi:10.5194/amt-3-1647-2010, 2010. 1541, 1567

Ungermann, J., Blank, J., Lotz, J., Leppkes, K., Hoffmann, L., Guggenmoser, T., Kaufmann, M., Preusse, P., Naumann, U., and Riese, M.: A 3-D tomographic retrieval approach with advection compensation for the air-borne limb-imager GLORIA, Atmos. Meas. Tech., 4, 2509–2529, doi:10.5194/amt-4-2509-2011, 2011. 1541

Ungermann, J., Kalicinsky, C., Olschewski, F., Knieling, P., Hoffmann, L., Blank, J., Woiwode, W., Oelhaf, H., Hösen, E., Volk, C. M., Ulanovsky, A., Ravegnani, F., Weigel, K., Stroh, F., and Riese, M.: CRISTA-NF measurements with unprecedented vertical resolution during the RECONCILE aircraft campaign, Atmos. Meas. Tech., 5, 1173–1191, doi:10.5194/amt-5-1173-2012, 2012. 1538, 1548

Ungermann, J., Pan, L. L., Kalicinsky, C., Olschewski, F., Knieling, P., Blank, J., Weigel, K., Guggenmoser, T., Stroh, F., Hoffmann, L., and Riese, M.: Filamentary structure in chemical

tracer distributions near the subtropical jet following a wave breaking event, Atmos. Chem. Phys., 13, 10517-10534, doi:10.5194/acp-13-10517-2013, 2013. 1540
Vogel, B., Pan, L. L., Konopka, P., Günther, G., Müller, R., Hall, W., Campos, T., Pollack, I., Weinheimer, A., Wei, J., Atlas, E. L., and Bowman, K. P.: Transport pathways and signatures of mixing in the extratropical tropopause region derived from Lagrangian model simulations, J. Geophys. Res.-Atmos., 116, D05306, doi:10.1029/2010JD014876, 2011. 1544, 1545
Vogel, B., Günther, G., Gross, J. U., Müller, R., Hoor, P., Müller, S., Krämer, M., and Riese, M.: Eastward Eddy Shedding from the Asian Monsoon Anticyclone and associated Transport Pathways of Boundary Layer Sources to the Stratosphere in September 2012, Atmos. Chem. Phys. Discuss., in preparation, 2014.
von Hobe, M., Bekki, S., Borrmann, S., Cairo, F., D'Amato, F., Di Donfrancesco, G., Dörnbrack, A., Ebersoldt, A., Ebert, M., Emde, C., Engel, I., Ern, M., Frey, W., Genco, S., Griessbach, S., Grooß, J.-U., Gulde, T., Günther, G., Hösen, E., Hoffmann, L., Homonnai, V., Hoyle, C. R., Isaksen, I. S. A., Jackson, D. R., Jánosi, I. M., Jones, R. L., Kandler, K., Kalicinsky, C., Keil, A., Khaykin, S. M., Khosrawi, F., Kivi, R., Kuttippurath, J., Laube, J. C., Lefèvre, F., Lehmann, R., Ludmann, S., Luo, B. P., Marchand, M., Meyer, J., Mitev, V., Molleker, S., Müller, R., Oelhaf, H., Olschewski, F., Orsolini, Y., Peter, T., Pfeilsticker, K., Piesch, C., Pitts, M. C., Poole, L. R., Pope, F. D., Ravegnani, F., Rex, M., Riese, M., Röckmann, T., Rognerud, B., Roiger, A., Rolf, C., Santee, M. L., Scheibe, M., Schiller, C., Schlager, H., Siciliani de Cumis, M., Sitnikov, N., Søvde, O. A., Spang, R., Spelten, N., Stordal, F., Sumińska-Ebersoldt, O., Ulanovski, A., Ungermann, J., Viciani, S., Volk, C. M., vom Scheidt, M., von der Gathen, P., Walker, K., Wegner, T., Weigel, R., Weinbruch, S., Wetzel, G., Wienhold, F. G., Wohltmann, I., Woiwode, W., Young, I. A. K., Yushkov, V., Zobrist, B., and Stroh, F.: Reconciliation of essential process parameters for an enhanced predictability of Arctic stratospheric ozone loss and its climate interactions (RECONCILE): activities and results, Atmos. Chem. Phys., 13, 9233–9268, doi:10.5194/acp-13-9233-2013, 2013. 1540
Weigel, K., Riese, M., Hoffmann, L., Hoefer, S., Kalicinsky, C., Knieling, P., Olschewski, F., Preusse, P., Spang, R., Stroh, F., and Volk, C. M.: CRISTA-NF measurements during the AMMA-SCOUT-O3 aircraft campaign, Atmos. Meas. Tech., 3, 1437–1455, doi:10.5194/amt-3-1437-2010, 2010. 1540
Weigel, K., Hoffmann, L., Günther, G., Khosrawi, F., Olschewski, F., Preusse, P., Spang, R., Stroh, F., and Riese, M.: A stratospheric intrusion at the subtropical jet over the Mediter-

AMTD
7, 1535–1572, 2014
GLORIA scientific objectives
M. Riese et al.

ranean Sea: air-borne remote sensing observations and model results, Atmos. Chem. Phys., 12, 8423–8438, doi:10.5194/acp-12-8423-2012, 2012. 1540
Werner, A., Volk, C. M., Ivanova, E. V., Wetter, T., Schiller, C., Schlager, H., and Konopka, P.: Quantifying transport into the Arctic lowermost stratosphere, Atmos. Chem. Phys., 10, 11623–11639, doi:10.5194/acp-10-11623-2010, 2010. 1548
Wetzel, G., Oelhaf, H., Kirner, O., Ruhnke, R., Friedl-Vallon, F., Kleinert, A., Maucher, G., Fischer, H., Birk, M., Wagner, G., and Engel, A.: First remote sensing measurements of ClOOCl along with ClO and $ClONO_2$ in activated and deactivated Arctic vortex conditions using new ClOOCl IR absorption cross sections, Atmos. Chem. Phys., 10, 931–945, doi:10.5194/acp-10-931-2010, 2010. 1548
Wetzel, G., Oelhaf, H., Kirner, O., Friedl-Vallon, F., Ruhnke, R., Ebersoldt, A., Kleinert, A., Maucher, G., Nordmeyer, H., and Orphal, J.: Diurnal variations of reactive chlorine and nitrogen oxides observed by MIPAS-B inside the January 2010 Arctic vortex, Atmos. Chem. Phys., 12, 6581–6592, doi:10.5194/acp-12-6581-2012, 2012. 1548
Wiegele, A., Kleinert, A., Oelhaf, H., Ruhnke, R., Wetzel, G., Friedl-Vallon, F., Lengel, A., Maucher, G., Nordmeyer, H., and Fischer, H.: Spatio-temporal variations of NO_y species in the northern latitudes stratosphere measured with the balloon-borne MIPAS instrument, Atmos. Chem. Phys., 9, 1151–1163, doi:10.5194/acp-9-1151-2009, 2009. 1548
Wirth, V.: Static stability in the extratropical tropopause region, J. Atmos. Sci., 60, 1395–1409, doi:10.1175/1520-0469(2003)060<1395:SSITET>2.0.CO;2, 2003. 1545
Woiwode, W., Oelhaf, H., Gulde, T., Piesch, C., Maucher, G., Ebersoldt, A., Keim, C., Höpfner, M., Khaykin, S., Ravegnani, F., Ulanovsky, A. E., Volk, C. M., Hösen, E., Dörnbrack, A., Ungermann, J., Kalicinsky, C., and Orphal, J.: MIPAS-STR measurements in the Arctic UTLS in winter/spring 2010: instrument characterization, retrieval and validation, Atmos. Meas. Tech., 5, 1205–1228, doi:10.5194/amt-5-1205-2012, 2012. 1539, 1540, 1548
Xiao, Y. P., Logan, J. A., Jacob, D. J. Hudman, R. C., Yantosca, R., and Blake, D. R.: Global budget of ethane and regional constraints on US sources, J. Geophys. Res.-Atmos., 113, D21306, doi:10.1029/2007JD009415, 2008. 1542

AMTD
7, 1535–1572, 2014

GLORIA scientific objectives

M. Riese et al.

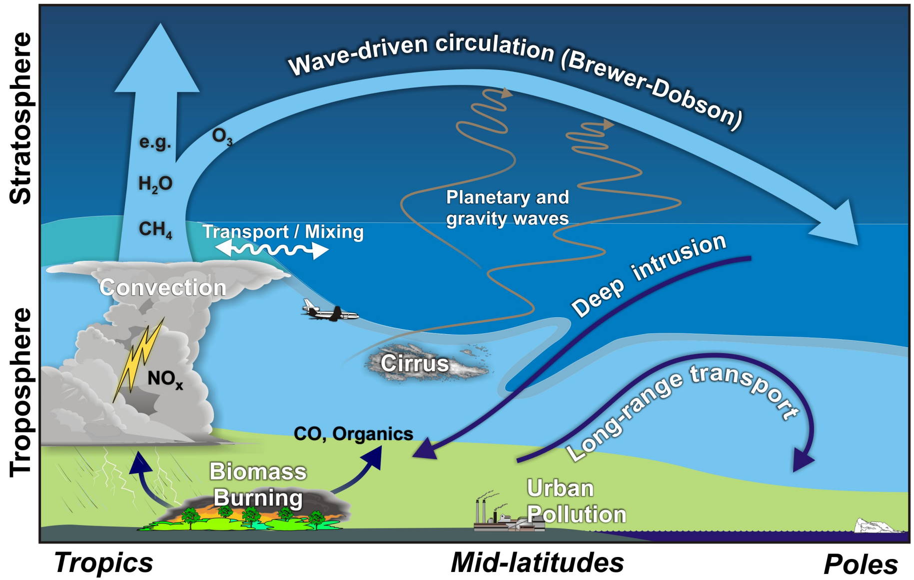

Fig. 1. Processes that determine UTLS composition. The middle shaded blue is the lowermost stratosphere (LMS), where isentropic surfaces cross the tropopause and facilitate quasi-horizontal transport (white wave-like arrow).

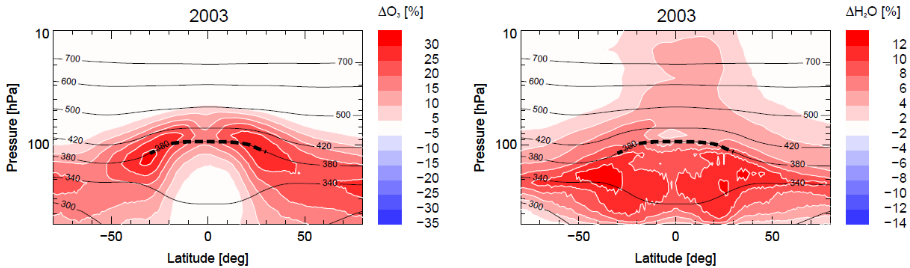

Fig. 2. Influence of uncertainties in the atmospheric mixing strength on simulated UTLS ozone (left) and water vapour (right). Shown are percentage differences for zonally averaged values (2003) obtained for two simulations with the Chemical Lagrangian Model of the Stratosphere (CLaMS), spanning the current uncertainty range of atmospheric mixing strength. For details see Riese et al. (2012).

AMTD
7, 1535–1572, 2014

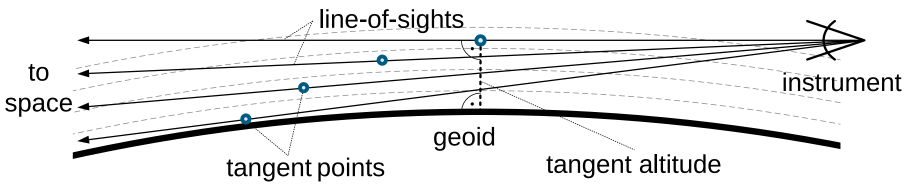

Fig. 3. Limb-viewing geometry for a limb sounder. The instrument measures the radiance emitted by the atmosphere along the line of sight (LOS). The LOS altitude that is closest to the Earth surface is the tangent altitude, the corresponding point is the tangent point. The limb-viewing geometry yields relatively good vertical resolution as a result of the spherical geometry and the exponential decrease of atmospheric density with altitude. GLORIA records radiance from all LOS simultaneously.

AMTD
7, 1535–1572, 2014

Title Page
Abstract | Introduction
Conclusions | References
Tables | Figures
◀| |▶
◀ ▶
Back | Close
Full Screen / Esc
Printer-friendly Version
Interactive Discussion

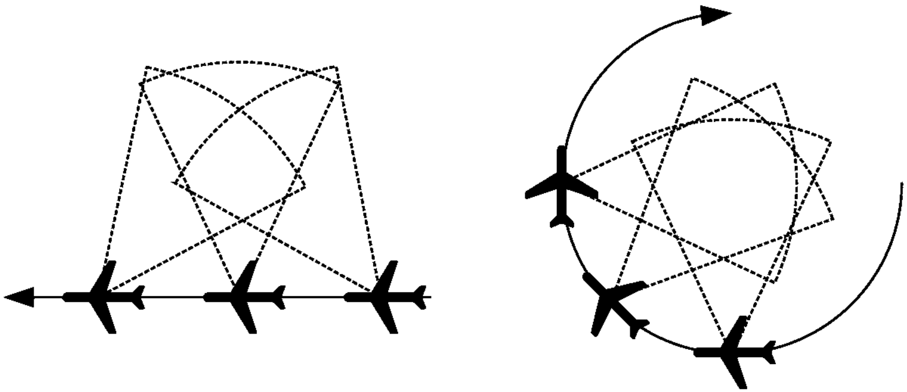

Fig. 4. Flight patterns of GLORIA onboard HALO or M55-Geophysica. The panning range of the instrument is illustrated by dashed lines. Line-of-sight (LOS) panning allows already for tomographic measurements during linear flights (left), since a fraction of the air volume covered is observed from different directions. The tomographic capabilities can be further enhanced by chosing a closed flight pattern like a circle (right).

AMTD
7, 1535–1572, 2014

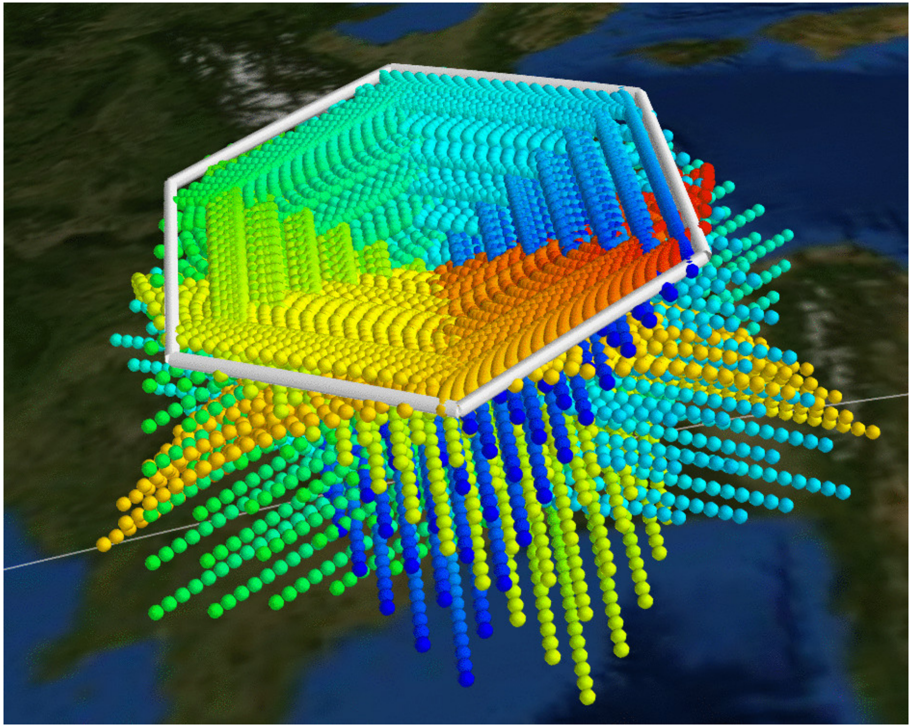

Fig. 5. Visualisation of a hexagonal flight pattern and corresponding tangent points. Each color corresponds to limb-observations obtained for one flight segment. For example, red points correspond to measurements made during the first flight segment and blue points correpond to measurements made during the last flight segment. The tangent point density is highest in a 2–3 km thick layer below the flight level. For details see (Ungermann et al., 2010).

AMTD
7, 1535–1572, 2014

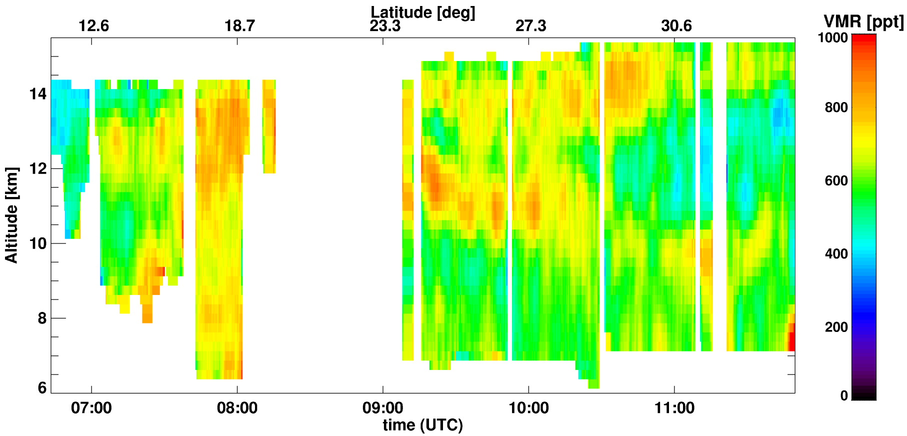

Fig. 6. Distribution of ethane (C_2H_6) derived from GLORIA chemistry mode measurements along the track of flight 18 September 2012 over the Arabian Sea and the Arabian Peninsula. For noise reduction and better visibility of the major signatures the original distribution with 13 s resolution has been smoothed using a running mean over two minutes.

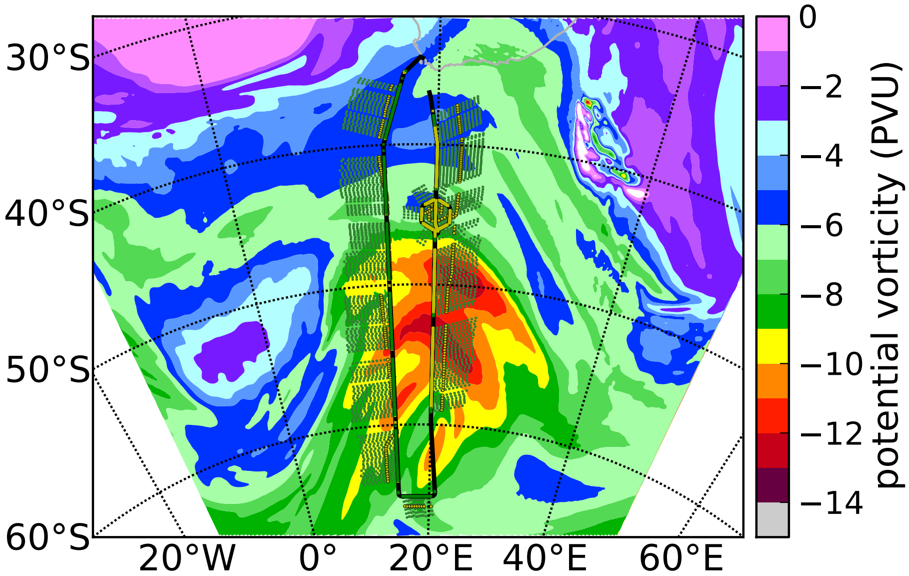

Fig. 7. Meteorological situation during the ESMVal flight on 12 September 2012. Coloured areas indicate potential vorticity (PV) values at 12 km altitude. The flight path is shown by the coloured line. Operation phases in the dynamics mode and chemistry mode are shown in yellow and green, respectively. The tomographic measurement, indicated by the hexagon, was made in an area of strong wave activity as reflected in the PV field.

AMTD
7, 1535–1572, 2014

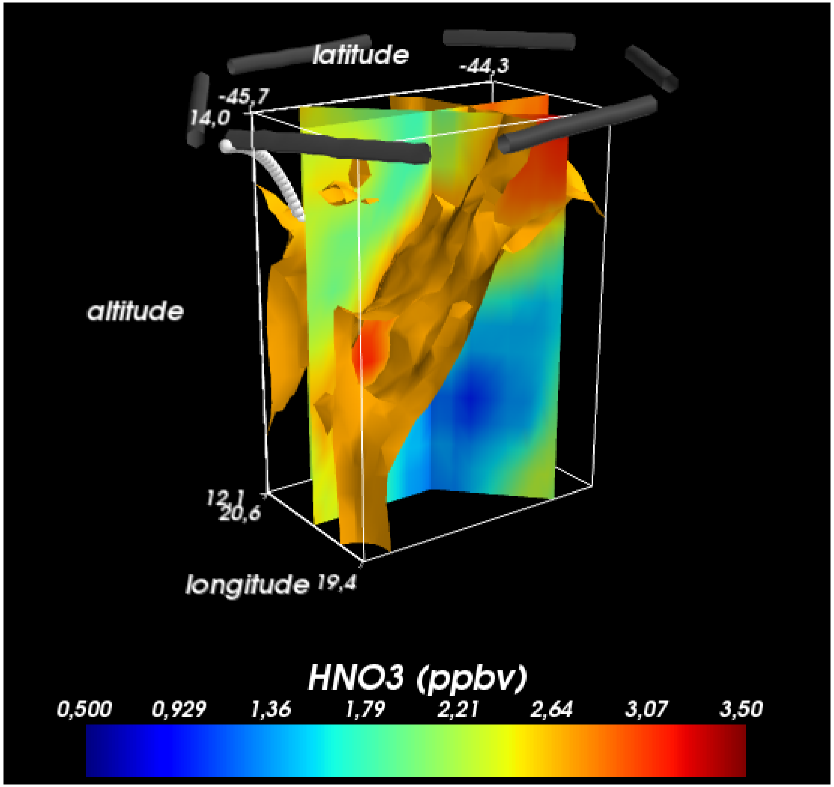

Fig. 8. First tomographic observation of a three-dimensional small-scale structure during a HALO flight on 12 September 2012. The HALO flight track at about 14 km is indicated by dark grey bars. The tomographic measurement volume extends down to about 12 km. Individual tangent points are presented by small white spheres. The most prominent feature is a filament of stratospheric air (enhanced HNO_3 values) that is surrounded by tropospheric air. The filament is illustrated by the 2.7 ppbv contour of enhanced HNO_3 values. In addition, some cross sections of HNO_3 values through the tomographic volume are displayed.

AMTD
7, 1535–1572, 2014

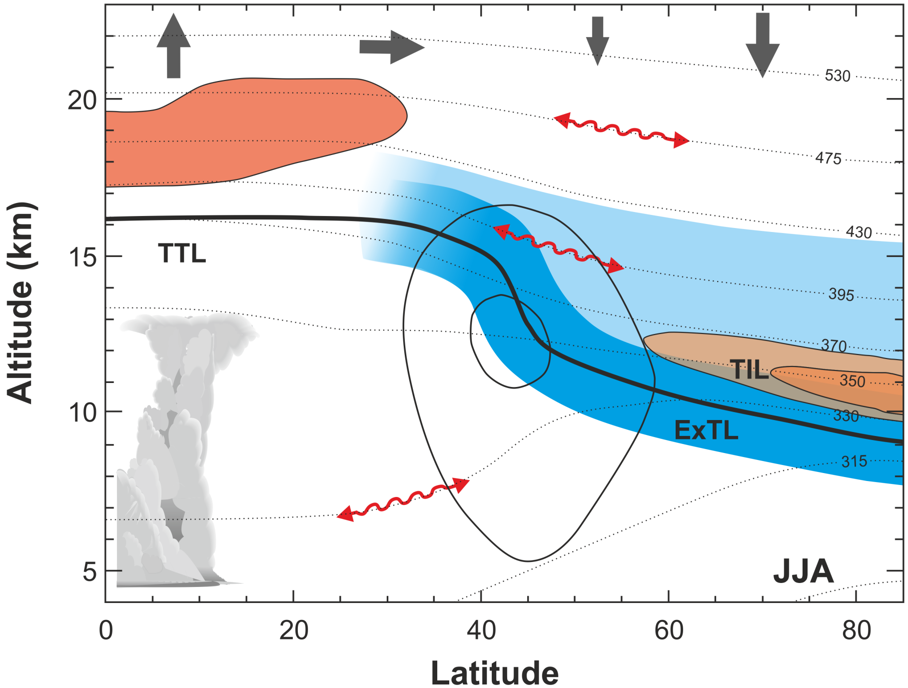

Fig. 9. Illustration of dynamical and chemical structure of the UTLS for Northern Hemisphere summer (JJA) conditions (adapted from Fig. 2b of Gettelman et al., 2011). The thick black line represents the thermal tropopause for the period 2002 to 2008. Dotted lines are isentropes. Black solid contours indicate the location of the subtropical jet (STJ). Areas of enhanced static stability (tropopause inversion layer) are indicated by red color shading. The Extratropical Transition Layer (ExTL) is represented in dark blue and the lowermost stratosphere (LMS) above the ExTL in light blue.

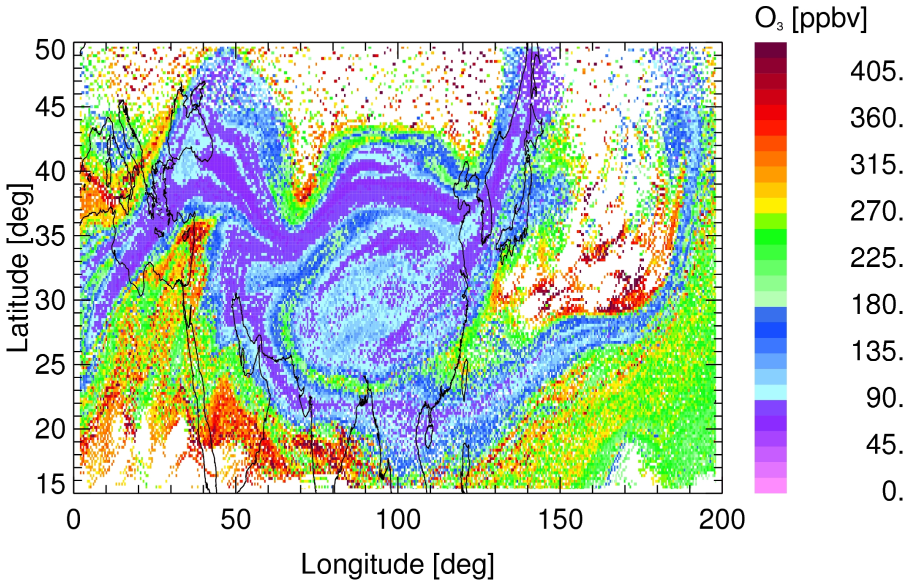

Fig. 10. Ozone distribution in the upper part of the Asian monsoon anti-cyclone (about 18 km) for 9 August 2003 as simulated by the CLaMS model with a horizontal resolution of around 25 km. The Asian monsoon has a strong influence on the composition of the tropical tropopause region (TTL). "Young" tropospheric air (low ozone) results from fast convective upward-transport in the centre of the Asian monsoon. Quasi-horizontal mixing of older extra-tropical stratospheric air (high ozone values) into the TTL occurs at the edge of the highly variable anticyclone.

AMTD
7, 1535–1572, 2014

GLORIA scientific objectives

M. Riese et al.